*Journal of Ceramic Processing Research. Vol. 23, No. 4, pp. 466~475 (2022)*
*(Received 17 January 2022, Received in revised form 22 February 2022, Accepted 23 February 2022)*
*https://doi.org/10.36410/jcpr.2022.23.4.466*

J O U R N A L O F
**Ceramic Processing Research**

# A study on tensile strength mechanism of hypoeutectic gray cast iron reinforced by composite silicon carbide powder

**Chunfeng Wang[a,b], Jun Yang[a], Guilin Liu[a,*], Hong Gao[a] and Meiling Chen[a]**
[a]*School of Materials Science and Engineering, Dalian Jiaotong University, Dalian, 116028, China*
[b]*Guangxi Yuchai Machinery Co., Ltd. Yulin 537005, China*

**This study aims to reveal the changes in the microstructure of hypoeutectic gray cast iron under the addition of composite silicon carbide powder of different mass fractions, and to explore how modified silicon carbide (SiC) particles of different sizes and contents improve the mechanical properties of hypoeutectic gray cast iron. The results showed that the modified SiC particles increased the nucleation, the undercooling and microstructure of hypoeutectic gray cast iron, and the tensile strength of the iron at room temperature was increased by 18,28%. The present work solves the problem that traditional SiC ceramic particles are prone to agglomeration in molten metal, analyzes its action mechanism, and can expand the application of SiC ceramic particles to strengthening metal properties of casting materials.**

**Keywords: Composite SiC powder, Hypoeutectic gray cast iron, Microstructure, Tensile strength, Undercooling.**

## Introduction

Gray iron castings have been the dominating form of castings in industrial production due to the excellent properties of gray iron: low manufacturing cost, superb machinability, great wear resistance, and shock absorption [1-3]. The mechanical properties of gray cast iron are directly affected by its microstructure. The increasing global demand for high-quality, lightweight, and energy-saving machinery and equipment has encouraged extensive research on the development of low-cost and high-strength gray cast iron materials. In order to ensure mechanical properties, gray cast iron is generally hypoeutectic.

Adding trace ceramic particles to improve the metal properties of coating materials can help reduce the cost of producing high-quality castings, and has drawn wide research attention in these years. Over the past few years, various carbon and ceramic particles have been used as reinforcement materials. The mechanical properties of materials [4-8] are improved by using different preparation processes [8-14] and particles of different types [13-17], sizes [16-19] and forms [18,20]. Among them, SiC particles are outstanding, whose addition can improve the strength, wear resistance, and toughness of the material to varying degrees during material preparation [21-25]. Therefore, it is often used to strengthen gray cast iron, and its role in strengthening gray cast iron varies with its mode of addition and quality. According to some studies, SiC can be added to molten iron following iron inoculation, replacing FeSi as a silicon carrier in the whole casting temperature range. As a result, there is a change in thermal properties and its microstructure, as well as an increase in fluidity. Studies on the microstructure indicate that SiC makes the graphite distribution more uniform and increases the content of type A graphite. SiC can also refine eutectic clusters. During solidification, SiC tends to decay slowly in the molten cast iron [26-28]. Poluboyarov et al. added a trace of SiC to hypoeutectic gray cast iron through the in-mold inoculation method to increase the pearlite content and improve graphite morphology and mechanical properties [29]. Li et al. added SiC to gray cast iron by placing SiC particles at the bottom of the ladle, and then filled the ladle with molten iron for ten minutes. It was found that after adding SiC particles, the pearlite content was increased, and the mechanical properties and wear resistance were significantly improved [30]. The above research shows that SiC particles can improve the wear resistance and tensile strength of gray cast iron. It is worth noting that existing works mainly focused on the effect of SiC particles on the mechanical properties and microstructure of gray cast iron, but few explored the mechanism by which the particles strengthened the properties of gray cast iron. However, revealing the mechanism is necessary to extend the adoption of SiC ceramic particles in strengthening the properties of metal materials. Only by studying the mechanism can we achieve accurate control in engineering application of SiC ceramic particles and ensure quality of the final products.

Therefore, this paper studies the thermodynamic pro-

*Corresponding author:
Tel : +86-13457603693
E-mail: lgl@djtu.edu.cn

perties of the dissolution process of modified SiC in molten iron, and explores the mechanism by which modified SiC particles with different sizes and contents improve the hypoeutectic structure and tensile strength of gray cast iron. The research here is intended to provide a theoretical basis for optimizing the process in which modified silicon carbide particles improve the mechanical properties of gray cast iron and for expanding the application of SiC ceramic particles in strengthening metal properties of coating materials.

## Materials and Methods

### Material Preparation

Scrap steel (50%), reheat iron (35%), and pig iron (15%) are the key raw materials used in this study. Table 1 shows the basic chemical composition. To reduce the influence of composition fluctuations on the test results, 400 kg of iron was melted in a medium-frequency coreless induction furnace with a rated capacity of 500 kg. Then, 100 kg molten iron was transferred to the medium-frequency coreless induction furnace with a rated capacity of 150 kg preheated in advance each time. While about 100 kg molten iron was poured into the 150 kg electric furnace, the modified composite SiC powder was added into the furnace and made evenly distributed via the heating and stirring functions of the medium frequency furnace. When the temperature of the molten iron reached 1,480-1,500 ºC, they were extracted from the 150 kg furnace. After inoculation with the SiCaBa inoculant, two groups of test rods with a diameter of 30 mm were poured at a temperature of 1,410-1,430 ºC. The raw material of the composite SiC powder is α-SiC. Other metallic materials were added by mechanical ball milling and high-energy activation. Four schemes were devised based on the weight of the added composite SiC powder: 0.00 wt.%, 0.05 wt.%, 0.10 wt.%, and 0.15 wt.%.

### Analytical Tests

The particle size of the composite SiC powder before and after modification was detected by Mastersizer 2000 laser particle size analyzer of Malvin company in Britain, and the effect of modification on composite SiC powder was analyzed by Empyrean X-ray diffractometer. Phase analysis was performed before and after SiC modification using an Empyrean-type PW1710 X-ray diffractometer. Three test bars were obtained for each pouring scheme to examine the tensile properties of modified SiC at room temperature with CMT5205, a microcomputer-controlled electronic universal testing machine. After preparing the tensile samples, the microstructure was analyzed by Zeiss Axio Observer D1 Manual inverted metallographic microscope. The scanning electron microscopy (SEM) observation was conducted by FEI Quanta FEG 250 SEM instrument, and the energy-dispersive X-ray spectroscopy (EDS) analysis was conducted by Oxford. Keyence VHX-1000E, a three-dimensional digital video electron microscope, was used to detect and analyze the tensile samples, observe the concavity and convexity of the surface of the samples according to the photos taken, and calculate the height differences of the fracture surface. NETZSCH STA 449 synchronous thermal analyzer is used to analyze the solidification process of molten iron.

## Results

### Composite SiC Powder

The test results of the particle size analysis of composite SiC powder by a particle size analyzer before and after modification are shown in Figs. 1-2, respectively. Comparing Fig. 1 with Fig. 2 reveals that the average particle size of composite SiC powder after modification decreased from 26.53 mm (size in the original state) to 9.51 mm. The particle size of 50% composite SiC powder decreased from 24.54 mm to 7.07 mm after modification. The maximum particle size before modification was 60.79 mm and was diminished to 29.33 mm. The specific surface area grew from 0.35 sq.m/c.c. to 1.78 sq.m/c.c., an increase of 408.57%.

The test results demonstrated that the particle size of composite SiC powder was significantly reduced after treatment, and the average particle size was more concentrated due to the action of mechanical force and the high-energy activator. Its specific surface area dramatically increased, which improved the surface activity of composite SiC powder.

Fig. 3 shows the SEM analysis and test results of composite SiC powder. It can be observed that the composite SiC powder before modification (i.e., in the original state) has large edges and corners, and the particles of the SiC powder are irregular. After modification, the roundness of the composite SiC powder is significantly improved, the edges and corners have disappeared, the distribution is close to circular, and the particle size of the powder is significantly reduced.

The XRD analysis test results of composite SiC powder are shown in Fig. 4: the XRD line width of SiC powder in the original state is between 0-4500 (Fig. 4(a)), and the line range of SiC after ball milling is between 0-22500 (Fig. 4(b)). It indicates that the ball milling treatment causes lattice distortion of SiC, the

**Table 1.** Basic chemical composition

| Element | C | Si | Mn | P | S | Fe |
|---|---|---|---|---|---|---|
| Catalogue | 3.2–3.3 | 1.8–2.0 | 0.75–0.85 | ≤0.06 | 0.06–0.10 | Equilibrium |

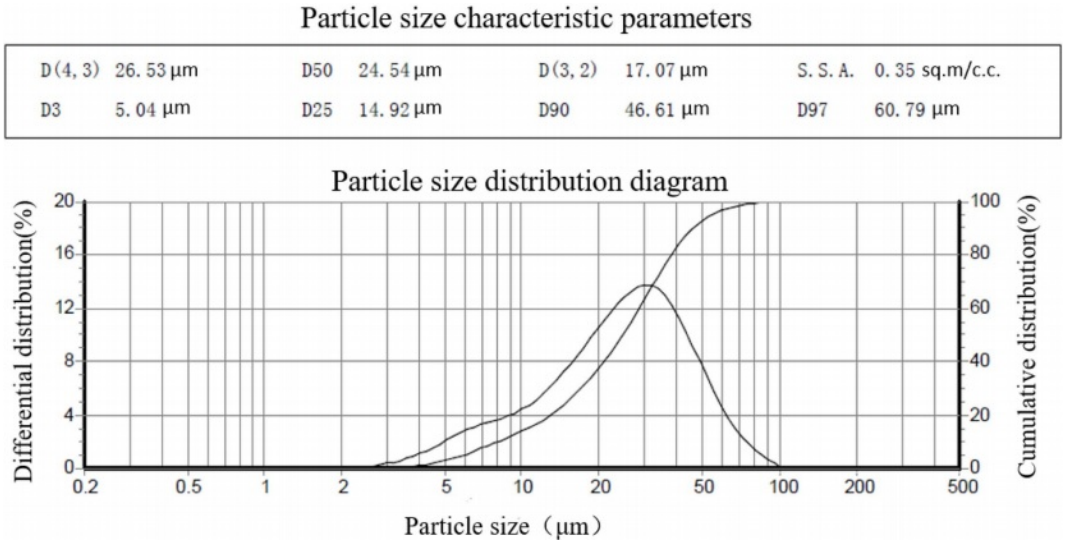


**Fig. 1.** Particle size distribution of original composite SiC.

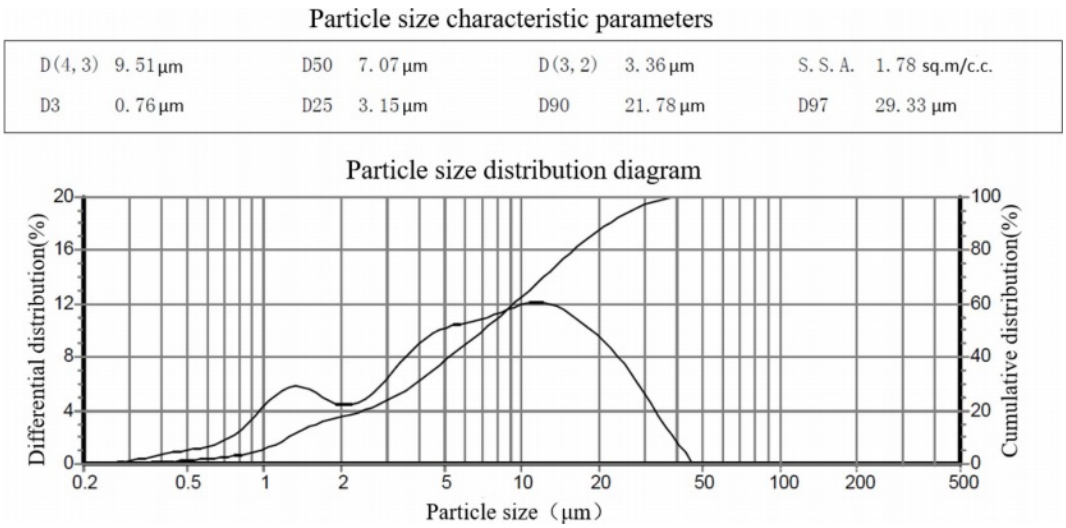


**Fig. 2.** Particle size distribution of composite SiC after modification.

powder has energy storage under the action of external force, and SiC itself is in a high-energy state. These findings are of great significance to analyze the action mechanism of SiC.

After the composite SiC powder was added to molten iron, the distribution and morphology of the powder were detected by SEM and EDS, as shown in Table 2 and Fig. 5. In the sample shown in Fig. 5-6, the small black particles are silicon carbide, which is mainly distributed in pearlite clusters and grain boundaries.

**Table 2.** The test results of EDS

| Element | Weight percent (wt.%) | Atomic percentage |
|---|---|---|
| C | 16.91 | 41.69 |
| Si | 27.24 | 28.71 |
| Fe | 55.84 | 29.6 |
| Total | 100.00 | 100.00 |

When the material is subjected to external tensile stress, the cells are stretched and broken to form fine cracks [31]. However, the presence of SiC in pearlite clusters and grain boundaries not only prevents the crack from expanding along its original grain boundary and grain path, but also avoids the connection and growth of adjacent fine cracks to a great extent.

Table 4 shows the differential distribution of the particle size and cumulative distribution of SiC in the composite SiC powder before being added to the molten gray cast iron. Statistical analysis shows that the particle size less than 1 μm accounts for 4.68% (i.e., cumulative distribution of SiC), 1-2 μm accounts for 12.80%, 2-5 μm accounts for 21.06%, and greater than 5 μm accounts for 61.44%. After adding composite SiC powder to the molten cast iron, the SiC particle size observed by SEM was calculated and compared with the particle size distribution listed in Table 3. As

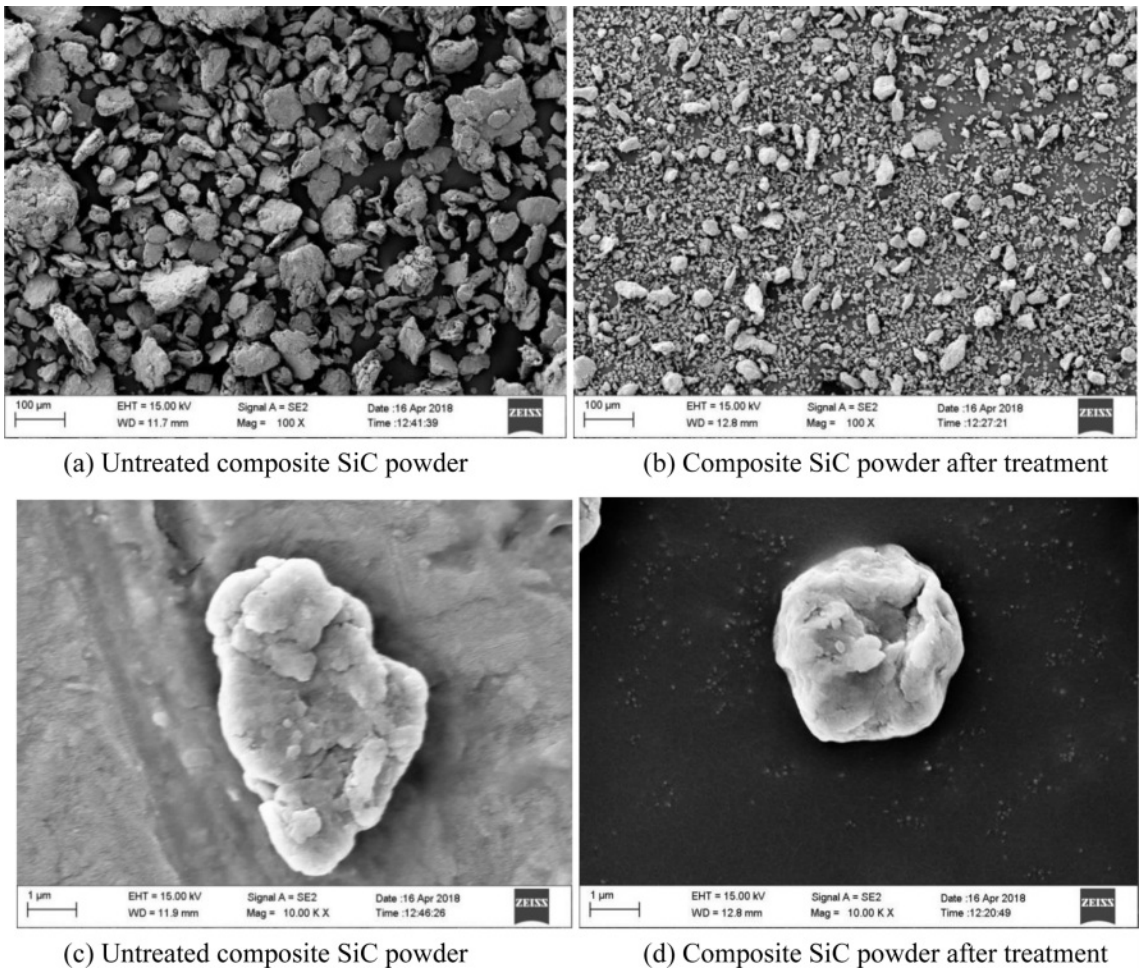


**Fig. 3.** Morphology of original composite SiC powder and modified composite SiC powder

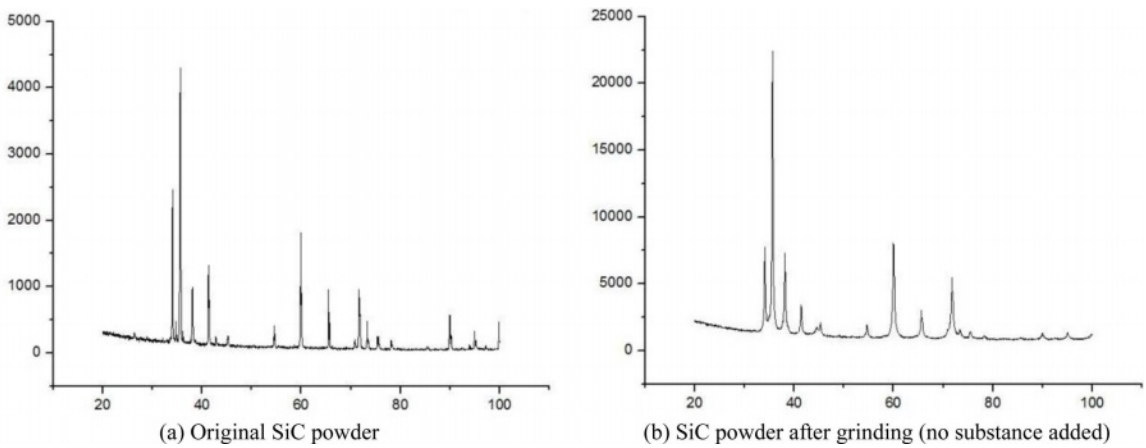


**Fig. 4.** The XRD test results of original SiC powder and ground SiC powder.

shown in Table 4, if the particle size is greater than 5 µm, the percentage of SiC powder decreased from 61.44% to 0.00% after being added to the molten cast iron. The percentage of SiC powder increased significantly in all three particle size ranges. If the particle size is less than 1 µm, the proportion of SiC powder increased from 4.68% to 20.83%. If the particle size was 1-2 µm, the proportion of SiC powder increased from 12.80% to 52.08%.

## Microstructure

As shown in Fig. 7, after addition of composite SiC particles, the graphite precipitated during solidification of hypoeutectic gray cast iron is basically type A. After

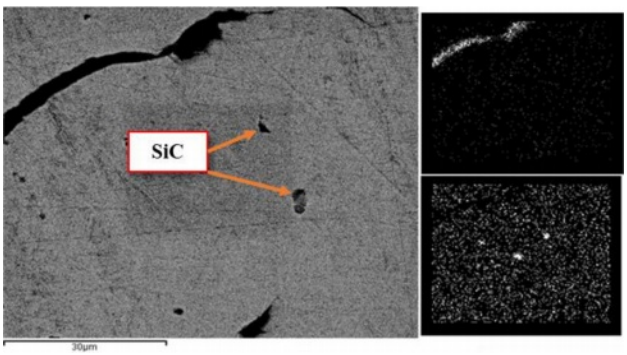


**Fig. 5.** Planar scanning of SiC particles.

addition of 0.00 wt.% composite SiC powder into the sample, the number of flake graphite was small, the shape is flat, and the length of graphite was 0.46 mm; after addition of 0.05 wt.% composite SiC powder, the number of graphite considerably increased, the length of graphite was 35 mm, and it was obviously bent; After addition of 0.10 wt.% powder, the number of graphite grew further, the length of graphite decreased to 30 mm, and the bending tendency was more obvious; After addition of 0.15 wt.% powder, the number of graphite was the largest, the length of graphite was the shortest, which was 20 mm, and the graphite showed

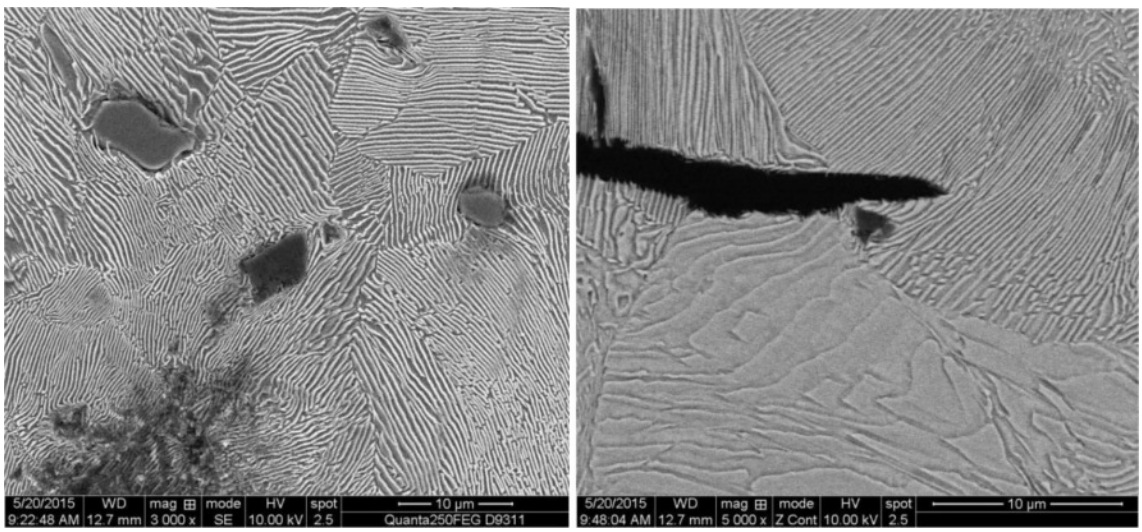

**Fig. 6.** Distribution and size of SiC particles.

**Table 3.** Particle size distribution of composite SiC powder

| Particle size (μm) | Differential distribution (%) | Cumulative distribution (%) | Particle size (μm) | Differential distribution (%) | Cumulative distribution (%) | Particle size (μm) | Differential distribution (%) | Cumulative distribution (%) |
|---|---|---|---|---|---|---|---|---|
| 0.20 | 0.00 | 0.00 | 2.89 | 3.07 | 23.01 | 38.00 | 0.87 | 99.65 |
| 0.24 | 0.00 | 0.00 | 3.50 | 4.38 | 27.39 | 41.84 | 0.14 | 99.79 |
| 0.29 | 0.07 | 0.07 | 4.24 | 5.82 | 33.21 | 50.00 | 0.20 | 99.99 |
| 0.35 | 0.20 | 0.27 | 5.00 | 5.32 | 38.54 | 50.64 | 0.00 | 99.99 |
| 0.43 | 0.44 | 0.71 | 6.21 | 7.18 | 45.71 | 54.00 | 0.00 | 99.99 |
| 0.52 | 0.60 | 1.31 | 7.51 | 6.41 | 52.13 | 61.28 | 0.00 | 100.00 |
| 0.63 | 0.77 | 2.07 | 9.09 | 6.80 | 58.93 | 74.17 | 0.00 | 100.00 |
| 0.76 | 0.93 | 3.00 | 10.00 | 3.73 | 62.67 | 89.76 | 0.00 | 100.00 |
| 0.92 | 1.67 | 4.68 | 13.53 | 11.78 | 74.45 | 108.63 | 0.00 | 100.00 |
| 1.11 | 2.77 | 7.44 | 16.11 | 6.25 | 80.70 | 131.47 | 0.00 | 100.00 |
| 1.35 | 4.24 | 11.69 | 19.50 | 6.13 | 86.83 | 159.11 | 0.00 | 100.00 |
| 1.63 | 3.29 | 14.97 | 23.60 | 5.46 | 92.29 | 192.57 | 0.00 | 100.00 |
| 1.97 | 2.50 | 17.47 | 28.56 | 4.13 | 96.42 | 233.06 | 0.00 | 100.00 |
| 2.39 | 2.47 | 19.94 | 34.57 | 2.36 | 98.78 | 282.06 | 0.00 | 100.00 |

**Table 4.** Particle size distribution of composite SiC powder before and after adding molten iron

| Particle size range of SiC | <1 μm | [1–2] μm | [2–5] μm | >5 μm |
|---|---|---|---|---|
| Before adding iron solution | 4.68% | 12.80% | 21.06% | 61.44% |
| After adding iron solution | 20.83% | 52.08% | 27.09% | 0% |

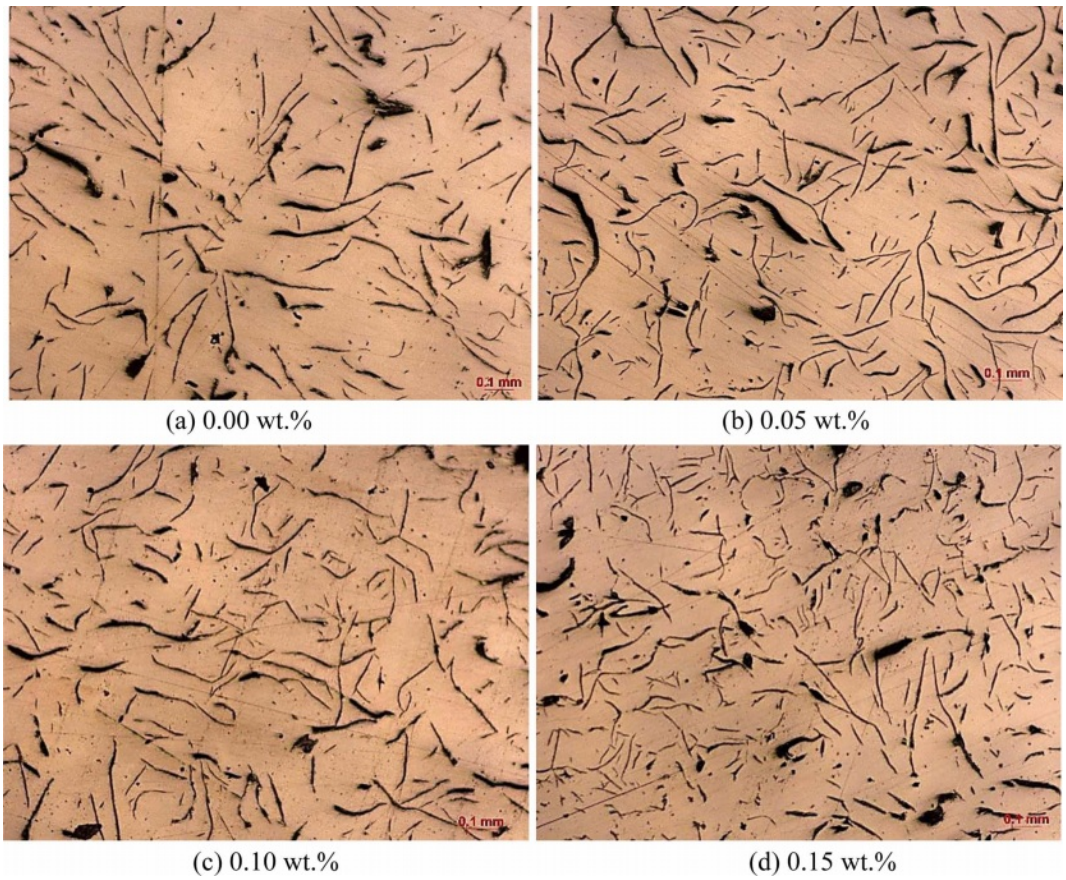


**Fig. 7.** Graphite morphology of tensile specimens of different amounts of composite SiC powder at room temperature.

more even distribution. With the increase of the amount of composite SiC powder, the graphite became finer and the number increased gradually. Finer and more evenly distributed graphite corresponds to higher tensile strength.

Fig. 8 shows the eutectic morphology of different composite SiC powders added after corrosion with 4% nitric acid ethanol solution. Without composite SiC powder, the eutectic grade of the sample was 7, and the grain was coarse and uneven (Fig. 8(a)). After addition of 0.05 wt.% composite SiC powder, the eutectic grade of the sample increased to 6, and the number of grains also increased (Fig. 8(b)). The eutectic grade rose to 5 after addition of 0.10 wt.% composite SiC powder, and the grains turned smaller (Fig. 8(c)). The eutectic grade of the sample with 0.15% composite SiC powder reached 4, with more grains and uniform grain size (Fig. 8(d)).

## Tensile Strength

In hypoeutectic gray cast iron, the test results of tensile strength with different addition amounts of composite SiC powder at room temperature are shown in Table 5. Addition of composite SiC powder significantly improved the tensile strength at room temperature, and the increase range of tensile strength grew with the amount of composite SiC powder. For example, the tensile strength of the composite SiC powder was enhanced by 12.82% after addition of 0.15 wt.% SiC powder.

The three-dimensional morphology of the tensile fracture of composite SiC powder with various mass fractions of SiC is shown in Fig. 9. The fracture surfaces of the four samples had different three-dimensional morphology (Fig. 9). The maximum protrusion height of the tensile fracture of the sample with 0 wt.% composite SiC powder was 596.4 mm (Fig. 9(a)), and the maximum bulge height of the tensile fracture with 0.05 wt.% composite SiC powder was 687.3 mm (Fig. 9(b)). Thus, the maximum height difference of tensile fracture increased by 15.24%. The maximum bulge height of the tensile fracture with 0.10 wt.% composite SiC powder was 753.8 mm. Thus, the vastest height difference of tensile fracture increased by 26.39%. The maximum protrusion height of tensile fracture added

**Table 5.** Effect of the content of composite SiC powder on tensile strength

| Addition amount of composite SiC powder (wt.%) | Tensile strength (MPa) | Increase range (%) |
|---|---|---|
| 0.00 | 273 | - |
| 0.05 | 286 | 4.76 |
| 0.10 | 305.5 | 11.90 |
| 0.15 | 308 | 12.82 |

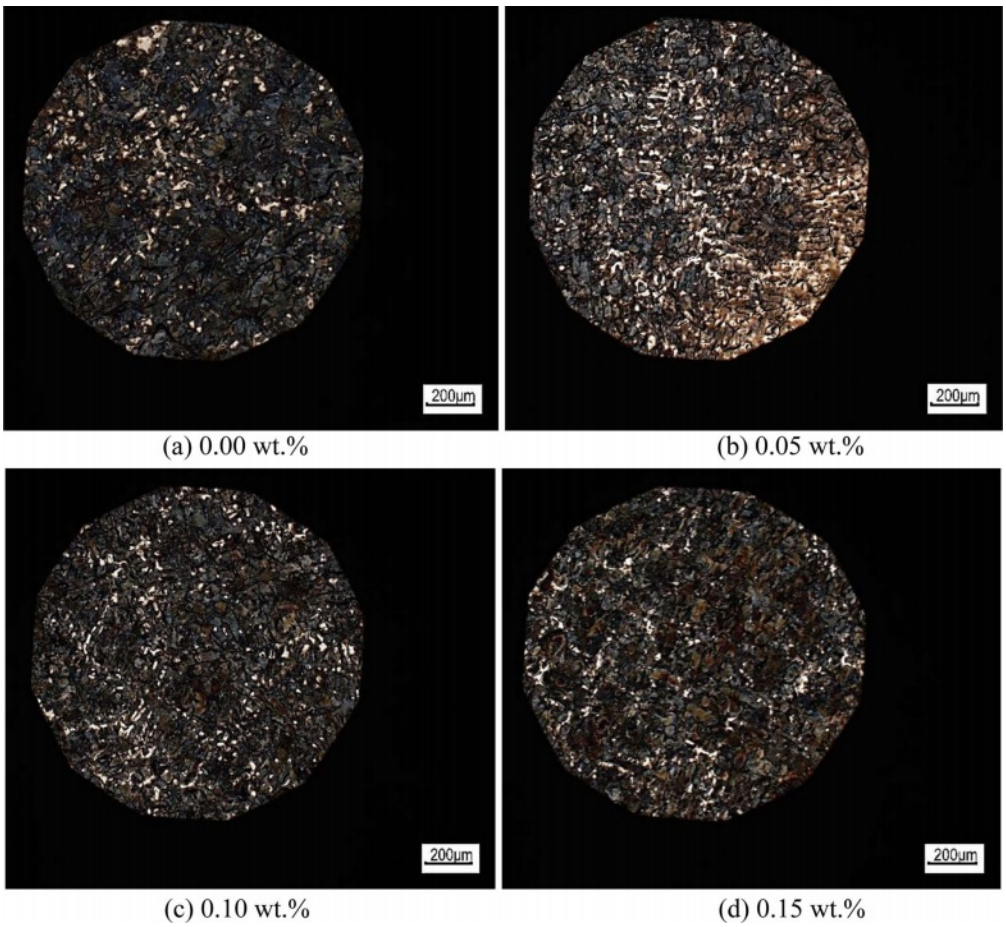


**Fig. 8.** Effect of gradient-modified SiC particle content on eutectic cells of hypoeutectic gray cast iron.

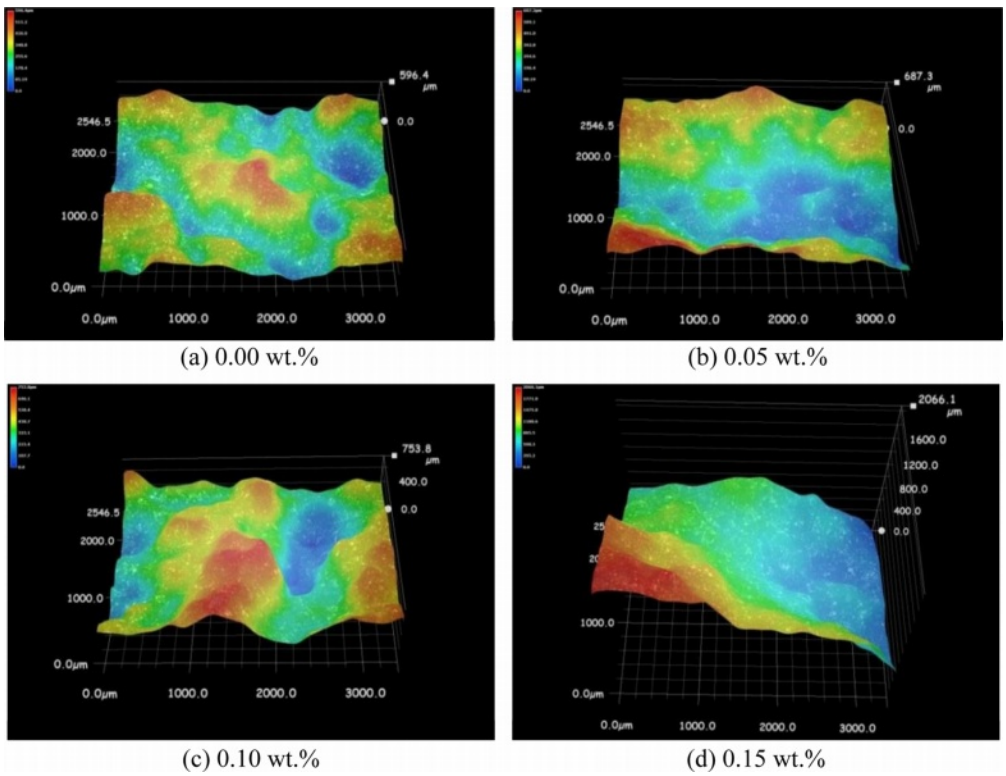


**Fig. 9.** Three-dimensional morphology with different mass fractions of composite powder.

**Table 6.** Results of DSC curve analysis for different addition amounts of composite SiC powder

| Addition amount of composite SiC powder (wt.%) | Liquidus temperature (°C) | Initial crystallization temperature (°C) | Undercooling (°C) | Undercooling difference (°C) | Increase (%) |
|---|---|---|---|---|---|
| 0.00 | 1216.7 | 1174.5 | 42.2 | | |
| 0.05 | 1216.7 | 1172.2 | 44.5 | 2.3 | 5.45 |
| 0.10 | 1216.7 | 1170.8 | 45.9 | 3.7 | 8.77 |
| 0.15 | 1216.7 | 1168.5 | 48.2 | 6 | 14.22 |

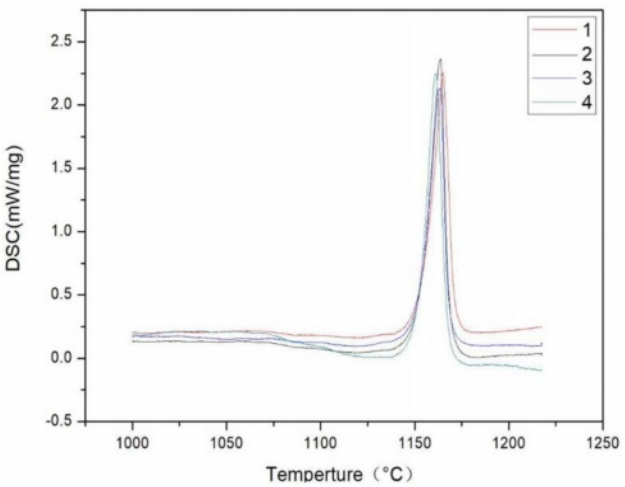


**Fig. 10.** The DSC curves of the different addition amounts of composite SiC powder: (1) 0.00 wt.%; (2) 0.05 wt.%; (3) 0.10 wt.%; (4) 0.15 wt.%.

with 0.15 wt.% composite SiC powder was 2,066.1 mm. Hence, the maximum height difference of tensile fracture increases by 246.43%.

### Thermal Analysis

Fig. 10 and Table 6 show the differential scanning calorimetry (DSC) curves and analysis results of different addition amounts of composite SiC powder. As demonstrated in Fig. 10, the starting temperature for crystallization decreases with the increasing amount of composite SiC powder. Consequently, the undercooling (i.e., the difference between initial crystallization temperature and liquidus temperature) of composite SiC powder increases with the amount of added composite SiC powder. When 0.05 wt.%, 0.10 wt.%, and 0.15 wt.% composite SiC powder was added, the undercooling of the powder increased by 2.3 °C, 3.7 °C, and 6 °C, respectively.

## Discussion

### Reaction of Composite SiC Powder in Molten Iron

Generally, SiC does not decompose and melt at normal atmospheric pressure; instead, it directly decomposes into gaseous Si at 2,760 °C. However, SiC can be gradually dissolved in molten iron. The dissolution process and free enthalpy are as follows [32]:

$$Si_{(L)} = [Si] \quad (1)$$

$$\Delta G^0 = 131377 - 17.2T \quad (2)$$

$$C_{(S)} = [C] \quad (3)$$

$$\Delta G^0 = 22572 - 42.2T \quad (4)$$

Therefore, in the cast-iron solution:

$$[Si]+[C]= SiC_{(S)} \quad (5)$$

$$\Delta G^0=3887 + 92.4T \quad (6)$$

As $\Delta G^0 >> 0$, the reaction can spontaneously proceed to the left. Hence, SiC can be decomposed into element [Si] and [C] in the molten cast iron, and the reaction cannot spontaneously proceed to the right. This indicates SiC particles are added rather than generated by the internal reaction, as shown in Figs. 5-6.

SiC can react in the molten cast iron:

$$SiC + Fe = FeSi + C \quad (7)$$

$$\Delta G^0 = 9900 - 9.14T \quad (8)$$

When T > 1083K, the reaction can spontaneously proceed to the right. At the melting temperature of cast iron, the reaction continues in the cast-iron solution. It is inferred that the size of SiC becomes smaller because of the continuous reaction in molten cast iron. This is consistent with the statistical results given in Table 5.

### Mechanism of composite SiC powder strengthening properties of hypoeutectic gray cast iron

In this study, SiC in composite SiC powder is α-SiC, a hexagonal crystalline form. The lattice constant of the (001) plane is 3.08 Å, and that of the graphite (0001) plane is 2.46 Å. The lattice mismatch between SiC and graphite is:

$$\delta = \frac{|a_c - a_s|}{a_c} \times 100\% = \frac{|3.08 - 2.46|}{3.08} \times 100\% \approx 20\%$$

Here, δ is less than 25%, so SiC can be used as the nucleation core of graphite to a certain extent. Some literature [33] shows that as a heterogeneous crystal nucleus precipitated from graphite, its size is less than 5 mm (generally 1-2 mm). The particle size distribution of SiC powder shown in Table 4, where 38.56% of SiC powder has a particle size of less than 5 mm, and 17.48% is less than 2 mm. Therefore, SiC powder below 5 mm can be used as the heterogeneous core of the graphite. Simultaneously, it can be seen from Formula

(8) that the reaction (7) will continue at the liquid to the solid transition temperature. Therefore, the non-equilibrium graphite precipitated by reaction (7) of SiC in the molten cast iron can be directly used as the nucleation core of the graphite. When the large particle size SiC decreases to 5 mm due to the reaction, it can also be directly used as the core of graphite nucleation. SiC plays the above three roles, so the number of eutectic clusters increases. Moreover, with the increasing number of eutectic clusters, the grain growth will be limited, and the grain can be refined.

Nucleation rate is used to characterize the number of nuclei formed per unit volume per unit time. The heterogeneous nucleation rate can be calculated as follows:

$$I = c \cdot \exp\left[-\left(\frac{B \cdot f(\theta) + U}{\Delta T^2}\right)\right], \quad (9)$$

where $f(\theta) = \frac{2 - 3\cos\theta + \cos^3\theta}{4}$ and $B = \frac{16\pi\sigma_{CL}^2 T^2}{3L^2 KT}$.

From Formula (9), it can be seen that the greater the undercooling, the greater the nucleation rate of heterogeneous nucleation, and the more the number of nucleation sites. It reveals that the addition of composite SiC powder can elevate the nucleation rate and the number of cores and refine the grains even when SiC is not used as the nucleation core. The result of increasing undercooling of composite SiC powder indicates that the large particle size SiC plays the role of "micro chill." After the composite SiC powder is added into the molten iron, its temperature increases and needs to absorb heat. According to the proportion of particle size distribution of composite SiC powder in Table 3, the number of SiC particles per gram of cast iron melt is $6.29\times10^7$, $12.6\times10^7$, and $18.9\times10^7$ when the addition amount of SiC powder is 0.05 wt.%, 0.10wt.%, and 0.15wt.%, respectively. A large number of SiC particles absorb the surrounding heat, causing local temperature fluctuations, which is reflected in the increase of undercooling.

## Conclusion

The effect of composite SiC powder, as a pretreatment agent, on the microstructure and tensile strength of hypoeutectic gray cast iron was studied. The strengthening mechanism of composite SiC powder on the tensile strength of hypoeutectic gray cast iron was analyzed, and the results of this study are summarized below:

First, analysis by an optical microscope shows that the addition of composite SiC powder is helpful to refine graphite, shorten its length, end passivation, significantly increases the number of eutectic clusters and the number of uniform particle sizes in the structure. Moreover, with the increasing amount of composite SiC powder, the changing trend of both becomes more prominent.

Second, the addition of composite SiC powder substantially improves the tensile strength of hypoeutectic gray cast iron. Moreover, the improvement is more evident with the increase of added SiC. The tensile strength increases by 12.82% when SiC particle content is 0.15 wt.%.

Third, by adding composite SiC powder to gray molten cast iron as a pretreatment agent, small-particle SiC and the reaction product C can be directly used as the core of the graphite, promote the number of eutectic groups, refine the grain size, and improve the tensile strength of hypoeutectic gray cast iron.

It is also found that during the addition and dissolution of composite SiC powder, large-particle SiC plays the role of micro cold iron, increases undercooling, improves the nucleation rate, and boosts nucleation.

The addition timing and process of SiC in cast iron melt are also important factors affecting its strengthening effect, which need to be further studied in the future. At the same time, we will continue to explore how SiC ceramic particles can enhance the properties of other metals in order to expand their application in practical production.

## References

1. V. Norman, P. Skoglund, D. Leidermark, and J. Moverare, Int. J. Fatigue. 88 (2016) 121-131.
2. L. Yong, Q. Wei, and S. Yong. Mater. Sci. 9[10] (2016) 815.
3. S.N. Grigoriev, A.S. Mettle, and S.V. Fedorov, Metal Corrosion Heat Treat. 54[1-2] (2012) 8-12.
4. V. Vijayakumar, P. Johnson, R. Whenish, A. Rajan, and V. H Wilson, J. Ceram. Process. Res. 22[4] (2021) 401-408.
5. J. Shen, W. Yin, Q. Wei, Y. Li, J. Liu, and L. An, J. Mater. Res. 28[13] (2013) 1835-1852.
6. Ł. Rogal, D. Kalita, A. Tarasek, P. Bobrowski, and F. Czerwinski, J. Alloys Comp. 708 (2017) 344-352.
7. S. Sulaiman, Z. Marjom, M.I.S. Ismail, M.K.A. Ariffin, N. Ashrafi, Encyclopedia project 184 (2017) 773-777.
8. A. Vaško, L. Hurtalova, M. Uhrič ik, E. Tillova, Materialwiss. Werkstofftech. 47[5-6] (2016) 436-443.
9. K. Ozturk, R. Gecu, and A. Karaaslan, Ceram. Int. 47[13] (2021) 18274-18285.
10. K. Ozturk, R. Gecu, and A. Karaaslan, Ceram. Int. 47[13] (2021) 18274-18285.
11. C. Qiu, Y. Su, J. Yang, X. Wang, B. Chen, Q. Ouyang, and D. Zhang, Composites, Part B 220(2021) 108996.
12. B. Lipowska, B. Psiuk, M. Cholewa, and Ł. Kozakiewicz, Arch. Foundry Eng. 17[1] (2017) 115-120.
13. Z. A. Cevik, A. H. Karabacak, M. Kok, A. Canakcı, S S. Kumar, and T. Varol, J. Comp. Mater. 55[19] (2021) 2657-2671.
14. R. Sivabalana, K.R. Thangaduraib, and K. Leninc, J. Ceram. Process. Res. 22[6] (2021) 605-614.
15. A. Ramanathan, P.K. Krishnan, and R. Muraliraja, Manuf. Process. 42 (2019) 213-245.
16. V.A. Poluboyarov, Z.A. Korotaeva, A.A. Zhdanok, and V.A. Kuznetzov, J. Sib. Fed. Univ. Eng. Technol. 9[1] (2016) 117-125.

17. Y.N. Zan, Y.T. Zhou, H. Zhao, Z.Y. Liu, Q.Z. Wang, D. Wang, W.G. Wang, B.L. Xiao, and Z.Y. Ma, Compos. B Eng. 183 (2020) 107674.
18. H. Singh, D. Kumar, and H. Singh, Compos. Mater. 55 (2020) 109-123.
19. W. Zhuang, L. Xie, G. Liu, and J. Liu, Int. J. Mod. Phys. B. 33[10] (2019) 8.
20. L. Ci and J. Bai, Adv. Mater. 16 (2004) 2021-2024.
21. C. Kaemkit, S. Niyomwas, and T. Chanadee, J. Ceram. Process. Res. 21[4] (2020) 460-464.
22. K.-H. Lee and K.-W. Nam, J. Ceram. Process. Res. 19[1] (2018) 75-79.
23. Y. Kim, C. Jang, and E.-S. Kim, J. Ceram. Process. Res. 15[5] (2014) 294-297
24. JJ. Han, Z.I. Wu, S. Cui, W.J. Li, and Y. Du, J. Ceram. Process. Res. 8[1] (2007) 74-77.
25. B. Babu Suresh, G. Chandramohan, C. Boopathi, T. Pridhar, and R. Srinivasan, J. Ceram. Process. Res. 19[1] (2018) 69-74.
26. K. Edalati, F. Akhlaghi, and M. Nili Ahmadabadi, J. Mater. Process. Technol. 160 (2005) 183-187.
27. W. Xue and Y. Li, J. Alloys Comp. 689 (2016) 408-415.
28. K. Edalati, F. Akhlaghi, and M. Nili-Ahmadabadi, Int. J. Cast Metal Res. 17[3] (2004) 147-151.
29. В.А. Полубояров, А. Коротаева. ВНУТРИФОРМЕННОЕ МОДИФИЦИРОВАНИЕ ЧУГУНОВ.ИССЛЕДОВАНИЕ ВЛИЯНИЯ МОДИФИКАТОРОВ НА ОСНОВЕ КАРБИДАКРЕМНИЯ НА ПРОЦЕССЫ КРИСТАЛЛИЗАЦИИ СЕРОГО ЧУГУНА. СООБЩЕНИЕ 1*. ИЗВЕСТИЯ ВЫСШИХ УЧЕБНЫХ ЗАВЕДЕНИЙ. ЧЕРНАЯ МЕТАЛЛУРГИЯ № 6, 2014.
30. J. Li, M. Chen, and H. Gao, Mech. Eng. Mater. 30[12] (2006) 56-59.
31. H. Run (Mugang), X. Qing, and H. Yanyong, Modern Castiron 3[03] (1985) 15-18+22.
32. X. Li, in “Effect of SiC nanoparticles on microstructure and properties of Q235 steel” (Shenyang University, 2009).
33. R. Shanzhi, W. Mengchun, et al., J. Harbin Univ. Sci. Technol. 2[2] (1982) 75-94.